DOI: 10.1109/JMEMS.2022.3199167

https://ieeexplore.ieee.org/document/9866786

Lock-In Amplified Fluorescence Spectroscopy in a Digital Microfluidic Configuration for Antibiotic Detection of Ciprofloxacin in Milk

Rahul Eswar, C. Harrison Brodie, *Graduate Student Member, IEEE*, and Christopher M. Collier, *Member, IEEE*

***Abstract*—Antibiotic detection in dairy is crucial, as introduction of antibiotics in food can lead to antibiotic resistance and cause allergic reactions in consumers. Dairy farmers risk monetary fines for shipping contaminated milk. Microfluidics is an appealing technology, as it is portable, can be implemented on-site, and is highly automated. This work presents a digital microfluidic dairy device for antibiotic detection. The digital microfluidic dairy device explores integration of a lock-in amplifier with droplet-based microfluidic techniques, being electrowetting actuation and droplet control. The lock-in amplifier setup is initially demonstrated for the fluorescent dye rhodamine B, to establish baseline operation. Ultimately, the lock-in amplifier setup is demonstrated for detection of ciprofloxacin in milk. The limit of detection is significantly lowered through the integration of the lock-in amplifier technology. Actuation of milk and water samples is shown, demonstrating full two dimensional control over the position of water and milk droplets, to enable a complete lab-on-a-chip system. The results show promise for modern dairy testing of antibiotic signatures.**

***Index Terms*—BioMEMS, digital microfluidics, droplet microfluidics**

I. Introduction

It is a common practice around the world to administer veterinary drugs to cattle for promoting growth and regulating breeding. Furthermore, antibiotics are routinely used to treat infections in livestock such as cattle [1], [2]. Consequently, residues of these antibiotics and their metabolites are prone to appearing in dairy products which can then have negative effects on human health including allergic reactions [2] and antibiotic resistance [3].

To protect public health, regulatory bodies enforce the testing of dairy milk for antibiotic residues [4]. Dozens of regulated antibiotics must fall under specified concentration limits in order for the milk to be permissible for human consumption [5]. The tests for antibiotic residues are traditionally performed at a laboratory where dairy farmers must ship their milk in large containers [6]. The critical flaw in this method is that dairy farmers are unable to test the milk as they collect it and are therefore vulnerable to collecting large batches of contaminated milk. Modern commercially available on-site dairy testing devices have long response times [7], [8] and complex manual test procedures [9] which make them unviable to use during the milk collection process. To address this need for an on-site dairy tester, microfluidic devices represent a promising research technology.

Microfluidic devices are miniaturized sensors that aim to replicate chemical analyses performed in a laboratory onto an integrated device; thus, these devices are often referred to as lab-on-a-chip devices. Advantages of implementing chemical analyses on a microfluidic device include portability, minimal reagent consumption, and high throughput [10]–[13]. Traditional microfluidic devices are based on continuous flow of reagent fluid through channels of micron-scale width.

In recent decades, an emergent branch of microfluidics known as digital microfluidics (DMF) has been actively studied [14]–[17]. The ability of DMF devices to transport, split and mix individual droplets of liquid samples across a digitized grid of electrodes provides a highly scalable lab-on-a-chip architecture [18]–[21]. The reconfigurability of DMF devices yields the potential to perform multiple parallelized chemical analyses on a single integrated device [22]. Digital microfluidics devices have found applications including point-of-care clinical diagnostics [23], [24], environmental testing [25], and biological cell culturing [26], [27].

Digital microfluidics is important in dairy testing for the following reasons. First, dairy microfluidics will require preprocessing, particularly when searching for the multiple antibiotics that would be present in a typical cattle treatment. Cattle are treated with a cocktail of (typically) three antibiotics

Manuscript received November x, 2021; Revised December x, 2021, accepted December x, 2021.

This work was supported in part by the Natural Sciences and Engineering Research Council of Canada under Grant RGPIN-2017-04022 and Canada Foundation for Innovation JELF-37389.

R. Eswar is an alumnus from the Collier Research Group at the University of Guelph, Guelph, ON, Canada (reswar@uoguelph.ca)

C. H. Brodie is a Ph.D. student at the University of British Columbia and graduate researcher with the Collier Research Group, School of Engineering, University of British Columbia, Kelowna, BC, Canada (hbrodie1@mail.ubc.ca).

C. M. Collier is the principal investigator of the Collier Research Group and is an assistant professor at the School of Engineering, University of British Columbia, Kelowna, BC, Canada (christopher.collier@ubc.ca)

[28]. Farmers will have knowledge of the specific antibiotics their cattle receive, as this information is provided from the veterinarian report, thus informing the fluoresence wavelengths of interest (being necessary for the optical detection of antibiotics in milk via fluorescence spectroscopy—as later described in this manuscript). Second, dairy microfluidics will require automation. In general, existing techniques like the Charm Rapid One-Step Assay (ROSA) and Delvotest T test [8], [9] are manually implemented. Given that the on-farm use by nontechnical-trained personal (i.e., farmers), automation is crucial. Digital microfluidics can program in the electrode coordinates as a function of time for the application of the voltage source. This automation is also important because these measurements must be made in a short period of time, e.g., the typical five minutes that a cow is in the milking parlour [29]. Manual tests, or use without the automation of the DMF actuation may not be within this specification. Third, dairy microfluidics will require highly parallel operations (e.g., the multiple antibiotic application described above). Digital microfluidics is well-suited to highly parallel operations, as droplets can be moved independently thus enabling highly parallel and high throughput analyses. Fourth, dairy microfluidics will require reconfigurability. This is provided by DMF as these systems can be loaded with any number of droplet path instructions. Therefore, in the likely event to a clog, the system can be reconfigured to navigate around such obstacles, and continue to function while waiting for servicing.

For DMF to be adapted for on-site dairy testing, the functionality to detect antibiotic residues from milk droplets and to actuate milk droplets must be demonstrated. Previous works applying continuous microfluidics to antibiotic detection in milk have used chromatography [30], [31] and electrophoresis [6], [32]–[36] to separate sample particles based on mass, charge, and chemical structure. The separated particles flow through narrow channels on the device for subsequent detection by fluorescence spectroscopy [6], [31], [33]–[36] or mass spectrometry [32], [37]–[39]. Although continuous flow devices are effective in sensing antibiotics, they face significant limitations including need for preprocessing of milk samples, excessively high voltages and the need for custom buffer solutions. To prevent clogging of narrow channels, milk samples must be centrifuged or filtered using laboratory equipment. The channels must then be rinsed for several minutes between each trial. These procedures require time, equipment, and manual attention, which is often unavailable for on-site applications.

To achieve fast response times and low detection limits, continuous microfluidics rely on high voltages in range of 14 kV – 30 kV [31]–[39]. Although voltages low as 500 V have been demonstrated, they sacrifice performance and sensitivity [6]. These kilovolt scale potentials are challenging to generate in a miniaturized on-site dairy tester. By contrast, DMF devices commonly operate under 400 V [40] which can be reliably produced by a voltage boost converter circuit [41]. Continuous flow devices also require carefully prepared and stored buffer solutions to be loaded in the channels for each trial [6], [31]–[39]. To summarize, modern continuous flow devices are unsuitable for on-site dairy testing due to dependence on laboratory equipment, long preparation times, and manual processes. Digital microfluidic devices provide valuable improvements in these areas.

The most widely used detection method in DMF biosensors is optical detection including absorbance and fluorescence spectroscopy [11]. Optical detection is well-suited to DMF devices due to being contact-free, miniaturize-able, and accessible. Being contact-free allows optical detectors to work with biological sample droplets without the risk of biofouling [42]. Optical equipment including light emitting diodes (LEDs), photodiodes and optical filters have the small footprints required to integrate with microfluidic systems. Compatibility with fiber optic waveguides has further shown miniaturization of optical detection in DMF devices [43], [44]. Optical detection is also well-suited to dairy testing as multiple regulated antibiotics are measurable by fluorescence spectroscopy [31], [33].

Digital microfluidic sensors commonly rely on label molecules which selectively bind to the target analyte and are more readily detected [11]. Analytes sometimes undergo autofluorescence (e.g., fluoroquinolones such as ciprofloxacin and levofloxacin [45]), and the use of a label is unnecessary. The use of label molecules can be undesirable due to cost and complexity, as a new label molecule is used for each target analyte [46]. If used with analytes requiring a label, DMF can achieve such preprocessing, avoiding use of trained personnel [47]. Dependence on personnel and lab facilities is not well-suited to on-site applications. Thus, the development of DMF devices is valuable.

This work addresses the functionality of antibiotic sensing for an on-site DMF dairy tester. We present an optical detection method for antibiotics in milk droplets. The presented method is enabled by lock-in amplified fluorescence spectroscopy. Detection is performed in milk droplets without need for chemical separation thereby demonstrating compatibility with modern DMF devices. This method is demonstrated by detection of the ciprofloxacin antibiotic in droplets of milk. The relationship between droplet volume and fluorescent intensity of ciprofloxacin is also investigated. We also demonstrate actuation through electrowetting with complete two dimensional control of milk and water droplets. The results of this work demonstrate a viable detection method for integration in a DMF dairy tester.

II. Framework and Device

A. Lock-In Amplification

The lock-in amplifier (LIA) is a scientific instrument used to measure weak signals from a noisy background in applications where signal-to-noise ratio (SNR) is low [48]. The LIA is able to take a noisy signal and compare it to a reference signal to selectively extract the weak signal oscillating at the reference frequency [49]. The instrument is fundamentally composed of two components: a phase sensitive detector (PSD) and a low pass filter.

The PSD is a critical component in a LIA. The two input signals to the PSD are the raw signal and the reference signal. The raw signal is the noisy signal where there exists some weak component signal of interest at a target frequency. The reference signal is a separate sinusoidal signal whose frequency is equivalent to the target frequency. Thus, the general form of the raw signal and reference signal can be represented by

$$X(t)_{\text{raw}} = V_{\text{raw}} \sin(2\pi f_{\text{raw}} t + \theta_{\text{raw}}) \tag{1}$$

and

$$X(t)_{\text{ref}} = V_{\text{ref}} \sin(2\pi f_{\text{ref}} t + \theta_{\text{ref}}) \ , \tag{2}$$

where V is amplitude, f is frequency, and θ is phase shift for the raw and reference signals, respectively. Equation (1) and equation (2) can also be given in the frequency domain as

$$X(f)_{\text{raw}} = \frac{\delta(f - f_{\text{raw}}) - \delta(f + f_{\text{raw}})}{2} \tag{3}$$

and,

$$X(f)_{\text{ref}} = \frac{\delta(f - f_{\text{ref}}) - \delta(f + f_{\text{ref}})}{2} \ , \tag{4}$$

respectively. Note that frequency domain equations are shown without accounting for phase shift for simplicity. The PSD passes the raw and reference signals through a frequency mixer. This is analogous to multiplying the time domain signals or performing a convolution in the frequency domain. The resulting output of the PSD is

$$Y(t) = \frac{1}{2} V_{\text{raw}} V_{\text{ref}} [\cos(2\pi f_{\text{raw}} t - 2\pi f_{\text{ref}} t + \theta_{\text{raw}} - \theta_{\text{ref}}) - \cos(2\pi f_{\text{raw}} t + 2\pi f_{\text{ref}} t + \theta_{\text{raw}} + \theta_{\text{ref}})] \tag{5}$$

in the time-domain or

$$Y(f) = \frac{1}{4}\big(\delta(f - a) + \delta(f + a) - \delta(f - b) - \delta(f + b)\big) \tag{6}$$

in the frequency domain where $a = f_{\text{raw}} - f_{\text{ref}}$ and $b = f_{\text{raw}} + f_{\text{ref}}$. Considering the condition that $f_{\text{raw}} = f_{\text{ref}}$, equations (5) and (6) show the output from the PSD has two frequency components; one at frequency of zero, and another at the sum frequency of the inputs. This output signal is conditioned by a low pass filter which attenuates signal components at the sum frequency and its harmonics. The final output from the LIA is a DC signal with amplitude proportional to the reference frequency amplitude in the raw signal.

B. Device

Figure 1 shows a schematic of the proposed ultimate device. In Fig. 1(a) the main components are shown separated, being the printed circuit board (PCB) DMF actuation and indium tin oxide (ITO) fluorescence sensing platforms (top in image), the photodiode apparatus (bottom left in image), and the ultraviolet (UV) LED apparatus (bottom right in image). The photodiode apparatus and the UV LED apparatus are used to achieve fluorescence. The DMF actuation and sensing platform is used for droplet actuation and as a transparent and conductive platform to perform fluorescence. In Fig. 1(b) the operation is shown, whereby the left milk droplet is positioned on the ITO fluorescence sensing platform, and the right milk droplet is positioned on the PCB DMF actuation platform. The left milk droplet can have UV strike it from above and fluorescence visible light through the ITO (transparent substrate) and optical bandpass filter (blue substrate) and be incident on the photodiode below. With such a setup, droplets can be moved between the ITO fluorescence sensing platform and the PCB DMF actuation platform, allowing high throughput and preprocessing.

The photodiode used in experiments is the DET 36A (Thorlabs, United States) silicon based photodiode. This photodiode is sensitive to light wavelengths in the range of 350 to 1100 nm. The photodiode is operated in photovoltaic mode to minimize dark current. The bandpass optical filter is placed beneath the ITO fluorescence sensing platform and above the photodiode to block the excitation wavelength and pass the longer fluorescent wavelength. The LED and optical filters are chosen depending on fluorescent characteristics of the analyte.

The SR830 LIA (Stanford Research Systems, United States) takes the signal from the photodiode and is used here for the presented lock-in based florescence spectroscopy experiments. The LIA took input current from the photodiode to its internal transimpedance amplifier configured with a gain of 10^6 V/A. Sensitivity of the LIA is set as 50 mV/nA. The time constant is set as 30 milliseconds. The slope of the internal low pass filter is set as 18 dB.

The DMF device is divided into two separate custom printed circuit boards connected by flat ribbon cables. The first board houses a 6 × 6 electrode grid where each electrode has a pitch of 2,750 μm and gap of 100 μm to adjacent electrodes. An interdigitated electrode geometry is used to maximize contact line length of the droplet with adjacent electrodes and maximize droplet velocity [50]. The board has four copper layers used to connect high-voltage traces by via-holes to each of the electrode pads. A 419D acrylic conformal coating (M.G. Chemicals, Canada) is applied and traces are designed to safely handle the required voltage. A stretched layer of parafilm is then fixed over the coated electrodes to form a smooth contact surface with the droplet. Silicone oil forms the hydrophobic layer. The second circuit board (not shown in Fig. 1) in the system houses the microcontroller and control components. The microcontroller is an Arduino Nano running a state-machine event driven firmware. The microcontroller receives commands over UART from a host PC running a custom graphical user interface. Commands received by the microcontroller over UART are

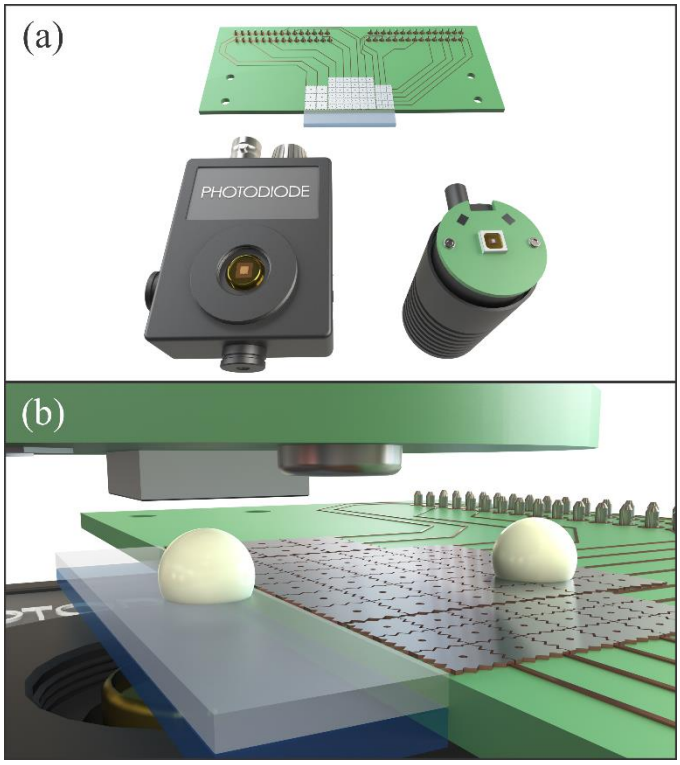

Fig. 1. The apparatus of the LIA fluorescence spectroscopy experiment is shown with (a) components separated and (b) components assembled together. In (a) the top image is the printed circuit board (PCB) digital microfluidic device (DMF) actuation platform and indium tin oxide (ITO) fluorescence sensing platform, the bottom left image is the photodiode, and the bottom right image is the ultraviolet (UV) light emitting diode (LED). In (b) the assembled proposed configuration of the experimental apparatus is shown. A microfluidic milk droplet is seen on the left between the UV LED and the ITO fluorescence sensing platform, with the photodiode beneath. A second microfluidic milk droplet is shown on the right that is positioned on the electrodes of the PCB DMF actuation platform, illustrating the parallel operational capability of the experimental apparatus.

translated to an HV507 serial-to-parallel converter chip for driving voltage to the electrodes. Electrodes are pulled to ground by default except for activated electrodes which are driven to 300 V DC.

Digital Microfluidic Lock-in Amplification

C. Pilot Experiment

A pilot experiment using the fluorescent dye rhodamine B (Sigma Aldrich) was performed to validate the experimental setup. The rhodamine B fluorescent dye emits visible light at a wavelength of 627 nm (i.e., red) when excited at 553 nm (i.e., green). The rhodamine dye is mixed in aqueous droplets to test concentrations ranging 0.5 µM to 67 µM. Droplets are pipetted onto the DMF dairy device at a fixed volume of 5.0 µL. A green LED is driven by a 2.5 kHz square wave from a function generator. The FEL0600 long-pass filter (Thorlabs, United States) with cut-on wavelength of 600 nm is used to pass only fluorescent light onto the photodiode. Between each trial the sample droplet is removed and a new droplet is pipetted. The photocurrent measured by the LIA versus rhodamine B concentration in aqueous droplets is plotted in Fig. 2, presented as a linear-linear plot in Fig. 2(a) and presented as a semi-log plot in Fig. 2(b).

The plot in Fig. 2 shows a positive correlation between fluorescent dye concentration and photocurrent. The logarithmic trend is characteristic of photodiodes operated in photovoltaic mode. The response can be made increasingly linear by reverse-biasing the photodiode and operating in the photoconductive mode although the drawback is increased dark current. The results of this pilot experiment validate performance of the experimental setup.

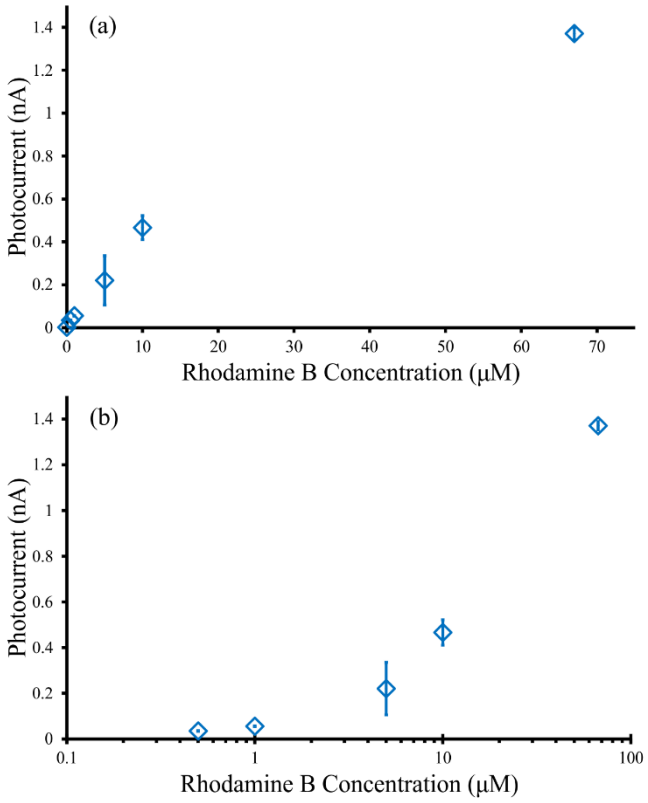

Fig. 2. Lock-in amplified photocurrent against rhodamine B concentration in 5.0 µL aqueous droplets. The mean photocurrent and corresponding standard deviation of n = 3 repeated measurements are shown as a function of rhodamine B concentration. The data is presented as (a) a linear-linear plot and (b) a semi-log plot. (Note that the (0,0) data point is omitted from the semi-log plot.)

D. Digital Microfluidic Antibiotic Detection

The following experiments measure concentration of ciprofloxacin in milk droplets on the ITO fluorescence sensing platform. Ciprofloxacin is a widely used antibiotic to treat cattle and is strictly regulated in dairy products [51]. Ciprofloxacin hydrochloride (Fisher Scientific, United States), is dissolved in two percent milk bought from a local vendor to produce solutions of concentrations ranging 0.01 mM to 1.00 mM. Previous studies demonstrated fluorescence of ciprofloxacin to emit at 440 nm (i.e., blue) when excited at 280 nm (i.e., ultraviolet) [52]. The LED used in this work is the commercially available VLMU60CL00-280–125 (Vishay

Semiconductors, United States) with peak wavelength of 280 nm and output power of 2.4 mW. The LED is driven by a 2.5 kHz square wave. The Edmund Optics 86–339 band-pass filter (Edmund Optics, United States) centered at 440 nm with bandwidth of 40 nm is placed above the photodiode. The photocurrent measured by the LIA is plotted against ciprofloxacin concentration in Fig. 3.

The results in Fig. 3 show an increasing photocurrent signal with increasing ciprofloxacin concentration in 5.0 µL of milk. The lowest ciprofloxacin concentration experimentally measured is 0.01 mM. The slope of the response curve in Fig. 3 corresponds to a measurement sensitivity of 1.39 nA/mM. The limit of detection can then be calculated as the ratio of three times the standard deviation of the blank reading to detection sensitivity [33]. This yields a limit of detection of 0.015 mM, producing an output that is statistically greater than the blank droplet reading. This 0.015 mM limit of detection achieved with LIA measurement is significantly improved from a similar experiment using continuous microfluidics and electrophoretic separation of milk with a limit of detection of 0.19 mM [6].

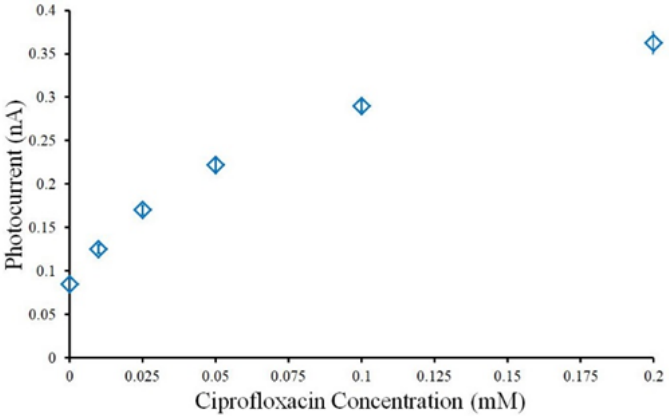

Fig. 3. Lock-in amplified photocurrent against ciprofloxacin concentration in 5.0 µL milk droplets. The mean photocurrent and corresponding standard deviation of n = 5 repeated measurements are shown as a function of ciprofloxacin concentration

E. Limit-of-Detection Considerations

In the literature there are more than one definition of the LOD equation. Sengul [53] summarizes the common LOD equations. The Visual Evaluation Method is described in equation (1) of Sengul. In the Visual Evaluation Method, the LOD is stated to be three times the standard deviation plus the average concentration. However, we follow the Signal-to-Noise Method, also reported on in Sengul, in equation (4). This Signal-to-Noise Method for the LOD equation is stated to be three times the standard deviation divided by the slope of the calibration curve.

F. Effect of Droplet Volume

The LIA fluorescent detection of ciprofloxacin in milk is performed with varied droplet volumes to investigate the effect on fluorescent output. These results are shown in Fig. 4. The results showed a general increase in LIA measured photocurrent with droplet volume which suggested increased fluorescent intensity with droplet volume. Previous studies have demonstrated that increased fluorescence intensity is not directly proportional to droplet volume [54]. Instead, the relation between droplet fluorescence intensity and volume is characterized by a complex interaction between scattering, ray focusing and absorbance within the droplet [55]. Handling large volumes would not be typical of a dairy application of the microfluidic chip. By comparison to closed configuration DMF, the open configuration is preferred as it is conducive to fluorescence spectroscopy with ultraviolet excitation and visible emission [56].

The LIA fluorescence spectroscopy method for measuring concentration of ciprofloxacin in milk droplets can be evaluated in terms of its limit of detection. Using fluorescence spectroscopy, a limit of detection of 0.015 mM for ciprofloxacin in milk droplets is achieved. At a molar mass of 331.35 g/mol and milk density of 1.03 kg/L, this limit of detection translates to 5 ppm which is comparable to the required regulatory limit of detection of 0.1 ppm [51]. This fluorescence spectroscopy detection can be extended to multiple antibiotics regulated in dairy milk.

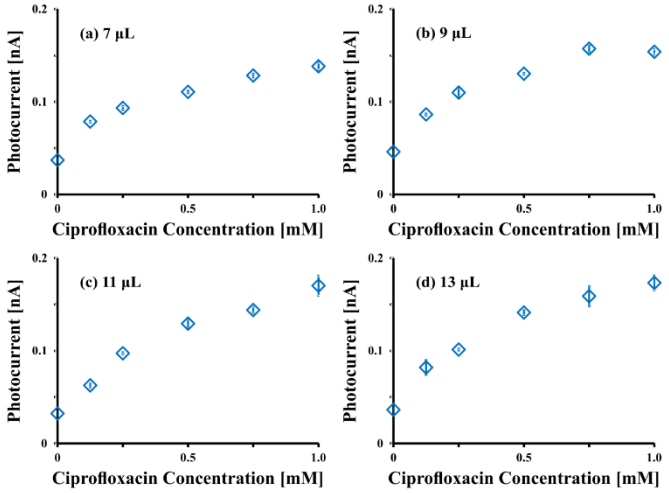

Fig. 4. Lock-in amplified photocurrent against ciprofloxacin concentration in milk droplets of volumes: (a) 7 µL, (b) 9 µL, (c) 11 µL and (d) 13 µL. The mean photocurrents and corresponding standard deviations of n = 3 repeated measurements are shown as a function of ciprofloxacin concentration.

G. Lock-in Amplification Considerations

The potential of a false positive measurement is discussed here. There have been some observances of fluorescence, e.g., Liu *et al.* noting fluorescence of raw milk at wavelengths of 350, 395, and 520 nm [57]. However, we use an optical bandpass filter with a narrow bandwidth of 40 nm and centre wavelength of 440 nm. This narrow bandpass filter ensures the other florescence described by Liu *et al.* is unlikely to be present on the photodiode. However, despite this protection being in place, further accounting for false positives is an important point of future work.

III. Digital Microfluidic Actuation

A. Digital Microfluidic Milk Droplet Actuation

The functioning of a full dairy lab-on-a-chip system requires open system actuation of milk droplets. This is shown in Fig. 5, where a milk droplet is actuated sequentially around a loop within a lab-on-a-chip DMF dairy device. This high level of control provides the potential for multiple LIA testing platforms within one lab-on-a-chip platform.

The DMF dairy device, with its PCB DMF actuation platform, can actuate multiple droplets simultaneously through programming of the via-hole electrodes. This is shown in Fig. 6, where the top droplet is milk and the bottom droplet is water. The droplets are originally positioned away from each other, then are actuated towards one another, and finally away again. Such operational control is required for analyte mixing.

B. Open and Closed Digital Microfluidic Systems

For this work, it is important to operate in a DMF open system, because the fluorescence requires the UV photons (e.g., 280 nm) to not pass through a glass top plate, due to its high optical absorption coefficient (greater than 1 cm^{-1}), while visible photons (e.g, 440 nm) can pass through a glass bottom plate, due to its low optical absorption coefficient (less than 0.01 cm^{-1}) [58]. Therefore an open system is important as the ITO glass is only present on the bottom of the droplet where there is visible light (440 nm) and not on the top of the droplet where there is UV (280 nm). Dispensing can be challenging for open systems. However, there is work done indicating that droplet splitting and manipulation can be achieved in an open system DMF chip [59].

IV. Conclusion

This work presented a lock-in amplifier measurement technique for a digital microfluidic device for dairy applications. The presented method is well-suited to integration on digital microfluidic devices. The work presented experimental results of actuation of milk and water droplets, with complete actuation control and programming. The results of this work are important to demonstrating a viable method for antibiotic detection in milk droplets which is necessary for future integration of microfluidic devices in the dairy industry.

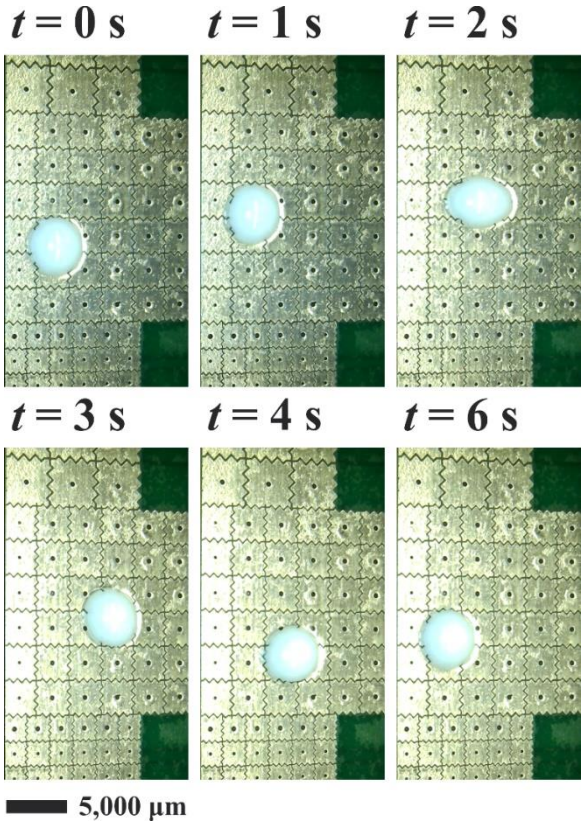

Fig. 5. The DMF actuation is shown on the DMF dairy device for a single milk droplet (approximately 2 µL) performing a square actuation pattern. The milk droplet ultimately returns to its starting position. Time steps are noted above each image frame.

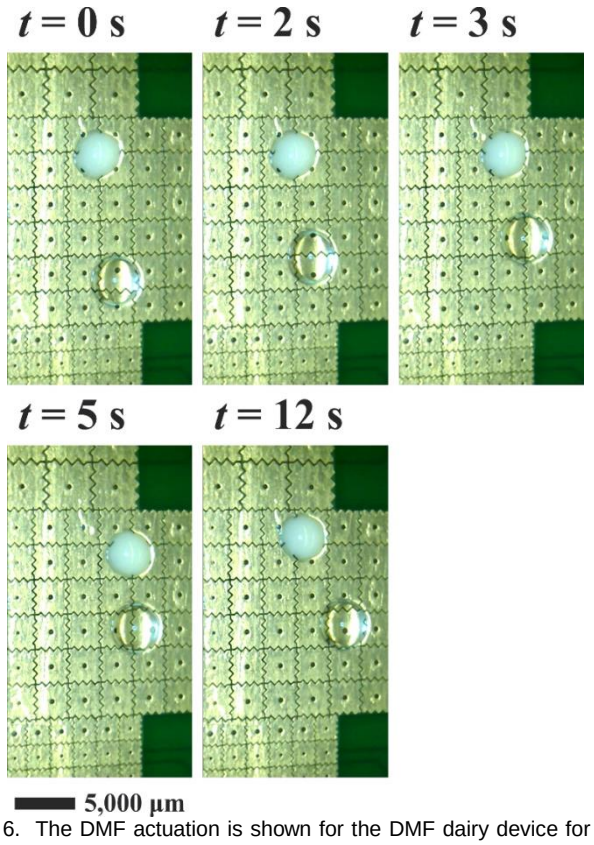

Fig. 6. The DMF actuation is shown for the DMF dairy device for two droplets, milk and water, performing an operation where the droplets initially move towards one another and then move apart.

REFERENCES

[1] O. A. Arikan, "Degradation and metabolization of chlortetracycline during the anaerobic digestion of manure from medicated calves," *J. Hazard. Mater.*, vol. 158, no. 2, pp. 485–490, 2008.

[2] A. Nisha, "Antibiotic Residues - A Global Health Hazard," *Vet. World*, vol. 2, no. 2, pp. 375–377, 2008.

[3] M. M. Hassan, K. Bin Amin, A. Mahabub Alam, S. Al Faruk, and I. Uddin, "Antimicrobial Resistance Pattern against E. coli and Salmonella in Layer Poultry*," Res. J. Vet. Pract.*, vol. 2, no. 2, pp. 30–35, 2014.

[4] H. Zhang, Y. Ren, and X. Bao, "Simultaneous determination of (fluoro)quinolones antibacterials residues in bovine milk using ultra performance liquid chromatography–tandem mass spectrometry," *J. Pharm. Biomed. Anal*., vol. 49, no. 2, pp. 367–374, 2009.

[5] J. M. Mitchell, M. W. Griffiths, S. A. McEwen, W. B. McNab, and A. J. Yee, "Antimicrobial Drug Residues in Milk and Meat: Causes, Concerns, Prevalence, Regulations, Tests, and Test Performance," *J. Food Prot.*, vol. 61, no. 6, pp. 742–756, 1998.

[6] R. Bosma, J. Devasagayam, A. Singh, and C. M. Collier, "Microchip capillary electrophoresis dairy device using fluorescence spectroscopy for detection of ciprofloxacin in milk samples," *Sci. Rep.*, vol. 10, no. 1, p. 13548, 2020.

[7] R. L. Althaus, A. Torres, A. Montero, S. Balasch, and M. P. Molina, "Detection Limits of Antimicrobials in Ewe Milk by Delvotest Photometric Measurements," *J. Dairy Sci.*, vol. 86, pp. 457–463, 2003.

[8] C. Bion, A. Beck Henzelin, Y. Qu, G. Pizzocri, G. Bolzoni, and E. Buffoli, "Analysis of 27 antibiotic residues in raw cow's milk and milk-based products – validation of Delvotest® T.," *Food Addit. Contam. Part A*, vol. 3, no. 1, pp. 54–59, 2016.

[9] M. C. Beltrán Martínez, R. Rueda, T. Althaus, R. Lisandro, and M. Pons, "Evaluation of the Charm maximum residue limit beta-lactam and tetracycline test for the detection of antibiotics in ewe and goat milk," *J. Dairy Sci.*, vol. 96, no. 5, pp. 2737–2745, 2013, doi: 10.3168/jds. 2012-6044.

[10] E. Samiei, M. Tabrizian, and M. Hoorfar, "A review of digital microfluidics as portable platforms for lab-on a-chip applications," *Lab Chip*, vol. 16, pp. 2376–2396, 2016, doi: 10.1039/c6lc00387g.

[11] M. G. Pollack, V. K. Pamula, V. Srinivasan, and A. E. Eckhardt, "Applications of electrowetting-based digital microfluidics in clinical diagnostics," *Expert Rev. Mol. Diagn.*, vol. 11, no. 4, pp. 393–407, 2011.

[12] A. C. Madison, M. W. Royal, and R. B. Fair, "Fluid Transport in Partially Shielded Electrowetting on Dielectric Digital Microfluidic Devices," J. Microelectromechanical Syst., vol. 25, no. 4, pp. 593–605, Aug. 2016.

[13] S. B. Puneeth and S. Goel, "Novel 3D Printed Microfluidic Paper-Based Analytical Device With Integrated Screen-Printed Electrodes for Automated Viscosity Measurements," IEEE Trans. Electron Devices, vol. 66, no. 7, pp. 3196–3201, Jul. 2019.

[14] M. G. Pollack, R. B. Fair, and A. D. Shenderov, "Electrowetting-based actuation of liquid droplets for microfluidic applications," *Appl. Phys. Lett.*, vol. 77, no. 11, pp. 1725–1726, Sep. 2000, doi: 10.1063/1.1308534.

[15] L. Luan, M. W. Royal, R. Evans, R. B. Fair, and N. M. Jokerst, "Chip Scale Optical Microresonator Sensors Integrated With Embedded Thin Film Photodetectors on Electrowetting Digital Microfluidics Platforms," IEEE Sens. J., vol. 12, no. 6, pp. 1794–1800, Jun. 2012.

[16] C. Li, W. Wang, L. Chao, X. Ji, and J. Zhou, "Detection of Faults and Barriers on Automated Large-Scale 2-D EWOD Digital Microfluidics," J. Microelectromechanical Syst., vol. 26, no. 6, pp. 1449–1456, Dec. 2017.

[17] A. Mohammadzadeh, A. E. Fox Robichaud, and P. R. Selvaganapathy, "Rapid and Inexpensive Method for Fabrication and Integration of Electrodes in Microfluidic Devices," J. Microelectromechanical Syst., vol. 28, no. 4, pp. 597–605, Aug. 2019..

[18] S. K. Cho, H. Moon, and C. J. Kim, "Creating, transporting, cutting, and merging liquid droplets by electrowetting-based actuation for digital microfluidic circuits," *J. Microelectromechanical Syst.*, vol. 12, no. 1, pp. 70–80, 2003, doi: 10.1109/JMEMS.2002.807467.

[19] C. M. Collier, M. Wiltshire, J. Nichols, B. Born, E. L. Landry, and J. F. Holzman, "Nonlinear dual-phase multiplexing in digital microfluidic architectures," *Micromachines*, 2011, doi: 10.3390/mi2040369.

[20] V. Jain and R. M. Patrikar, "A Low-Cost Portable Dynamic Droplet Sensing System for Digital Microfluidics Applications," IEEE Trans. Instrum. Meas., vol. 69, no. 6, pp. 3623–3630, Jun. 2020.

[21] A. Stephenson et al., "PurpleDrop: A Digital Microfluidics-Based Platform for Hybrid Molecular-Electronics Applications," IEEE Micro, vol. 40, no. 5, pp. 76–86, Sep. 2020.

[22] K. F. Böhringer, "Modeling and Controlling Parallel Tasks in Droplet-Based Microfluidic Systems," *IEEE Trans. Comput. Des. Integr. Circuits Syst.*, vol. 25, no. 2, pp. 334–344, 2006.

[23] R. Sista et al., "Development of a digital microfluidic platform for point of care testing," *Expert Rev. Mol. Diagn.*, vol. 8, no. 12, pp. 2091–2104, 2008.

[24] D. Millington, S. Norton, R. Singh, R. Sista, V. Srinivasan, and V. Pamula, "Digital microfluidics comes of age: high-throughput screening to bedside diagnostic testing for genetic disorders in newborns," *Expert Rev. Mol. Diagn.*, vol. 18, no. 8, pp. 701–712, 2018.

[25] Q. Zhang et al., "A feedback-controlling digital microfluidic fluorimetric sensor device for simple and rapid detection of mercury (II) in costal seawater," *Mar. Pollut. Bull.*, vol. 144, pp. 20–27, 2019.

[26] I. Barbulovic-Nad, S. H. Au, and A. R. Wheeler, "A microfluidic platform for complete mammalian cell culture," *Lab Chip*, vol. 10, no. 12, pp. 1536–1542, 2010.

[27] J. Zhai et al., "A digital microfluidic system with 3D microstructures for single-cell culture," *Microsystems Nanoeng*., vol. 6, no. 1, pp. 1–10, 2020.

[28] M Husien Yousif et al., "Low Concentration of Antibiotics Modulates Gut Microbiota at Different Levels in Pre-Weaning Dairy Calves," *Microorganisms*, vol. 6, no. 4, pp. 1–15, 2018.

[29] N. D. .Käppel, F. Pröll, and G. Gauglitz, "Low Concentration of Antibiotics Modulates Gut Microbiota at Different Levels in Pre-Weaning Dairy Calves," *Biosensors and Bioelectronics*, vol. 22, no. 9-10, pp. 2295–2300, 2007.

[30] Y. Zhao, M. Tang, F. Liu, H. Li, H. Wang, and D. Xu, "Highly Integrated Microfluidic Chip Coupled to Mass Spectrometry for Online Analysis of Residual Quinolones in Milk," *Anal. Chem.*, vol. 91, no. 21, pp. 13418–13426, 2019.

[31] V. H. Springer and A. G. Lista, "Micellar nanotubes dispersed electrokinetic chromatography for the simultaneous determination of antibiotics in bovine milk," *Electrophoresis*, vol. 33, no. 13, pp. 2049–2055, 2012.

[32] F. J. Lara, A. M. García-Campaña, F. Alés-Barrero, J. M. Bosque-Sendra, and L. E. García-Ayuso, "Multiresidue Method for the Determination of Quinolone Antibiotics in Bovine Raw Milk by Capillary Electrophoresis−Tandem Mass Spectrometry," *Anal. Chem.*, vol. 78, no. 22, pp. 7665–7673, 2006.

[33] G. Mu, H. Liu, L. Xu, L. Tian, and F. Luan, "Matrix solid-phase dispersion extraction and capillary electrophoresis determination of tetracycline residues in milk," Food Anal. Methods, vol. 5, no. 1, pp. 148–153, 2011.

[34] L. Vera-Candioti, A. C. Olivieri, and H. C. Goicoechea, "Development of a novel strategy for preconcentration of antibiotic residues in milk and their quantitation by capillary electrophoresis," *Talanta*, vol. 82, no. 1, pp. 213–221, 2010.

[35] S. M. Santos, M. Henriques, A. C. Duarte, and V. I. Esteves, "Development and application of a capillary electrophoresis based method for the simultaneous screening of six antibiotics in spiked milk samples," *Talanta*, vol. 71, no. 2, pp. 731–737, 2007.

[36] H. Sun, W. Zhao, and P. He, "Effective Separation and Simultaneous Determination of Four Fluoroquinolones in Milk by CE with SPE," *Chromatographia*, vol. 68, no. 5, pp. 425–429, 2008.

[37] C. Blasco, Y. Picó, and V. Andreu, "Analytical method for simultaneous determination of pesticide and veterinary drug residues in milk by CE-MS," *Electrophoresis*, vol. 30, no. 10, pp. 1698–1707, 2009.

[38] S. Wang, P. Yang, and Y. Cheng, "Analysis of tetracycline residues in bovine milk by CE-MS with field-amplified sample stacking," *Electrophoresis*, vol. 28, no. 22, pp. 4173–4179, 2007.

[39] D. Moreno-González, A. M. Hamed, B. Gilbert-López, L. Gámiz-Gracia, and A. M. García-Campaña, "Evaluation of a multiresidue capillary electrophoresis-quadrupole-time-of-flight mass spectrometry method for the determination of antibiotics in milk samples," *J. Chromatogr. A*, vol. 1510, pp. 100–107, 2017.

[40] V. Jain, T. P. Raj, R. Deshmukh, and R. Patrikar. "Design, fabrication and characterization of low cost printed circuit board based EWOD

device for digital microfluidics applications," *Microsyst. Technol.*, vol. 23, no. 2, pp. 389–397, 2017.
[41] M. Alistar and U. Gaudenz, "Opendrop: An integrated do-it-yourself platform for personal use of biochips," *Bioengineering*, 2017, doi: 10.3390/bioengineering4020045.
[42] E. Samiei, G. S. Luka, H. Najjaran, and M. Hoorfar, "Integration of biosensors into digital microfluidics: impact of hydrophilic surface of biosensors on droplet manipulation," *Biosens. Bioelectron*., vol. 81, pp. 480–486, 2016.
[43] K. Choi, J. M. Mudrik, and A. R. Wheeler, "A guiding light: spectroscopy on digital microfluidic devices using in-plane optical fibre waveguides," *Anal. Bioanal. Chem.*, vol. 407, no. 24, pp. 7467–7475, Sep. 2015, doi: 10.1007/s00216-015-8913-x.
[44] I. Spotts, D. Ismail, N. Jaffar, and C. M. Collier, "Fibre-optic sensing in digital microfluidic devices," *Sensors Actuators, A Phys.*, vol. 280, pp. 164–169, Sep. 2018, doi: 10.1016/j.sna.2018.07.039.
[45] A. B. Ikpe et al., "Evaluation of fertility response succeeding various therapeutic protocol in endometritic dairy cows under field condition," *The Pharma Innovation Journal*, vol. 10, no. 9, pp. 100–103, 2021.
[46] H. K. Hunt and A. M. Armani, "Label-free biological and chemical sensors," *Nanoscale*, vol. 2, no. 9, pp. 1544–1559, 2010.
[47] K. A. Neilson et al., "Less label, more free: Approaches in label-free quantitative mass spectrometry," *Proteomics*, vol. 11, no. 4, pp. 535–553, 2010.
[48] W. C. Michels and N. L. Curtis, "A Pentode Lock-In Amplifier of High Frequency Selectivity," *Rev. Sci. Instrum.*, vol. 12, no. 9, pp. 444–447, 1941.
[49] B. A. Colon, M. R. Hassan, A. Saleheen, C. A. Baker, and T. R. Calhoun, "Total Internal Reflection Transient Absorption Microscopy: An Online Detection Method for Microfluidics," J. Phys. Chem. A, vol. 124, no. 20, pp. 4160–4170, May 2020.
[50] V. Jain, V. Devarasetty, and R. Patrikar, "Effect of electrode geometry on droplet velocity in open EWOD based device for digital microfluidics applications," *Journal of Electostatics*, vol. 87, pp. 11–18, 2017.
[51] A. Aresta, P. Cotugno, and C. Zambonin, "Determination of Ciprofloxacin, Enrofloxacin, and Marbofloxacin in Bovine Urine, Serum, and Milk by Microextraction by a Packed Sorbent Coupled to Ultra-High Performance Liquid Chromatography," *Anal. Lett*., vol. 52, no. 5, pp. 790–802, 2019.
[52] R. Yang, Y. Fu, L. Di Li, and J. M. Liu, "Medium effects on fluorescence of ciprofloxacin hydrochloride," *Spectrochim. Acta - Part A Mol. Biomol. Spectrosc.*, 2003, doi: 10.1016/S1386-1425(03)00059-3.
[53] U. Sengul, "Comparing determination methods of detection and quantification limits for aflatoxin analysis in hazelnut," *J Food Drug Anal*, vol. 24, no. 1, pp. 56–62, 2016.
[54] R. Domann, Y. Hardalupas, and A. R. Jones, "A study of the influence of absorption on the spatial distribution of fluorescence intensity within large droplets using Mie theory, geometrical optics and imaging experiments," *Meas. Sci. Technol.*, vol. 13, no. 3, pp. 280–291, 2002.
[55] B. Frackowiak and C. Tropea, "Numerical analysis of diameter influence on droplet fluorescence," *Appl. Opt.*, vol. 49, no. 12, pp. 2363–2370, 2010, doi: 10.1364/AO.49.002363.
[56] I. Moon and J. Kim, "Using EWOD (electrowetting-on-dielectric) actuation in a micro conveyor system," *Sensors actuators. A. Phys*., vol. 130, pp. 537–544, 2006.
[57] H. Liu, W. Liu, D. Han, and S. Wang, "Detection of the Presence of Reconstituted Milk in Raw Milk and in Pasteurized Milk Using Synchronous Fluorescence Spectroscopy," *Food Analytical Methods*, vol. 10, pp. 2078–2084, 2017.
[58] A.-I. Bidegaray et al., "50 shades of colour: how thickness, iron redox and manganese/antimony contents influence perceived and intrinsic colour in Roman glass," *Archaeological and Anthropological Sciences*, vol. 12, 109(1-17), 2020.
[59] H. Geng, J. Feng, L. M. Stabryla, and S. K. Cho, "Droplet manipulations by dielectrowetting: Creating, transporting, splitting, and merging," *Proc. 2017 IEEE 30th International Conference on Micro Electro Mechanical Systems (MEMS)*, pp. 113-116, 2017.

Rahul Eswar received the B.Eng. degree in biomedical engineering and the M.A.Sc. degree in engineering systems and computing from the University of Guelph, Guelph, ON, Canada, in 2019 and 2021, respectively.

C. Harrison Brodie (M'17) received the B.Eng. degree in biomedical engineering and the M.A.Sc. degree in engineering systems and computing from the University of Guelph, Guelph, ON, Canada, in 2017 and 2019, respectively. He is currently working towards the Ph.D. degree in electrical engineering from the University of British Columbia, Kelowna, BC, Canada.

Christopher M. Collier (M'18) received the B.A.Sc. and Ph.D. degrees in electrical engineering from the University of British Columbia, Kelowna, BC, Canada, in 2011 and 2016, respectively. From 2016-2021, Dr. Collier was an Assistant Professor of Biomedical Engineering, University of Guelph, ON, Canada. He is currently an Assistant Professor of Electrical Engineering, School of Engineering, University of British Columbia, Kelowna, BC, Canada.